BIFURCATION ANALYSIS IN APOPTOSIS (RECEPTOR CLUSTERING)

SCIENCES DEPARTMENT THESIS FORMAT

A Thesis

Presented to the Faculty of the Department of Mathematical Sciences

Middle Tennessee State University

In Partial Fulfillment

of the Requirements for the Degree

Master of Science in Mathematical Sciences

---

by

Genesis Amelia Spears

June 2018

ABSTRACT

BIFURCATION ANALYSIS IN APOPTOSIS (RECEPTOR CLUSTERING)

Genesis Amelia Chavez Spears

Apoptosis is a designed cell death mechanism involved in biological processes. Apoptosis can either be activated by extrinsic pathway or by the intrinsic pathway. A major part of the external apoptosis pathway is the death receptor Fas which, on binding to its associated ligand FasL, they eventually form the death-inducing signaling complex. FasL promotes clustering for open Fas and activates open stable Fas, forming locally stable signaling platforms through neighborhood-induced receptor interactions. The model exhibits a bifurcation called hysteresis, providing an upstream mechanism for bistability and robustness to decide if the cell lives or dies. At low receptor concentrations, the bistability depends on three states of FasL. The irreversible bistability, representing a committed cell death decision, emerges at high receptor concentrations. Furthermore, the model suggests a mechanism by which cells may function as bistable life/death switches which are independent of their downstream dynamic components. This will be illustrated by simulations.

DEDICATION

To my son Timothy who has been with me through this entire journey of writing this thesis. Finding out I was pregnant with you as I was starting to write this thesis helped me see the meaning of diligent hands and working hard in a new light. I feel like we wrote this thesis together and you have brought so much happiness and joy in my life. I love you Timothy Nathan Spears and you can do and be anything God wants you to be or do. Spend time in His words and trust in Him.

ACKNOWLEDGMENTS

I would like to give a special thanks to my husband, Nathan Mark Spears, for his patience, unconditional support, love, encouragement, and believing in me. Also thanks to everyone in my family for their patience and love, especially my mother, who has been praying and encouraging me through the ups and downs of coming back to school.

I would also like to give my gratitude to my thesis advisor and mentor, Dr. Zachariah Sinkala for his patience, time, encouragement, knowledge, and experience. I would also like to thank the reviewing committee for their time reviewing this thesis.

Last, but not least, as a person of faith, a very special thank you and gratitude to my heavenly Father for providing in this season and teaching me about the meaning of sacrifice and hard work with love.

Contents

List of Figures

CHAPTER 1

INTRODUCTION

1.1 Overview

Apoptosis is a systematic cellular process of destroying cells in physiological and pathological conditions. It plays a significant role in many biological processes. The purpose of apoptosis is to remove unneeded cells, for example, cells with damaged DNA. Normal apoptosis plays a major role in development, tissue homeostasis, cell termination, and immune response. An abnormal apoptosis has been associated with a variety of diseases such as development defects, neurodegenerative disorders, autoimmune disorders, and cancer, see [8, 19, 24, 28, 29]. Because of its biological importance, much work has been devoted in understanding the biological pathways responsible for apoptosis. Recently, this has led to growth of mathematical models (mechanistic and integrative) to study apoptosis, see [1, 2, 3, 4, 7, 9, 18, 22]. These mathematical models have contributed new insights into understanding underlying molecular interactions involved in apoptosis. The current work takes a mathematical approach also. The mathematical analysis of our model will shed some more light into understanding apoptosis.

Apoptosis can be activated by one of two pathways: the extrinsic pathway (receptor-mediated signals from other cells) and the intrinsic pathway (mitochondrial-mediated signals within the cell). Because apoptosis is irreversible, it is a highly regulated process[15]. This work focuses on the central part of the extrinsic pathway (See Fig. 1) which is the death signal initiated from other cells such as FasL, a ligand that binds to its associate transmembrane death receptor, Fas. These clusters the intracellular

receptor death domains and promotes the connection of the Fas Associated Death Domain (FADD) to form the death-inducing signaling complex (DISC). The DISC causes the activation of caspases, the active caspases activate other inactive caspases in a chain reaction, to initiate apoptosis [12].

Apoptosis is viewed as a bistable system, with an all-or-nothing switch between local stable life and death equilibrium states[16]. Bistability plays an important role in the robustness of apoptosis. Computational models have emerged as tools to identify and study sources of bistability in apoptosis. For example: positive caspase feedback [7], inhibition of DISC by cFLIP [4], cooperativity in apoptosome formation [3], double-negative caspase feedback through XIAP [18], and double-negative feedback in Bcl-2 protein interactions [6]. In this work, we assume that bistability may be induced upstream by open and stable death receptors.

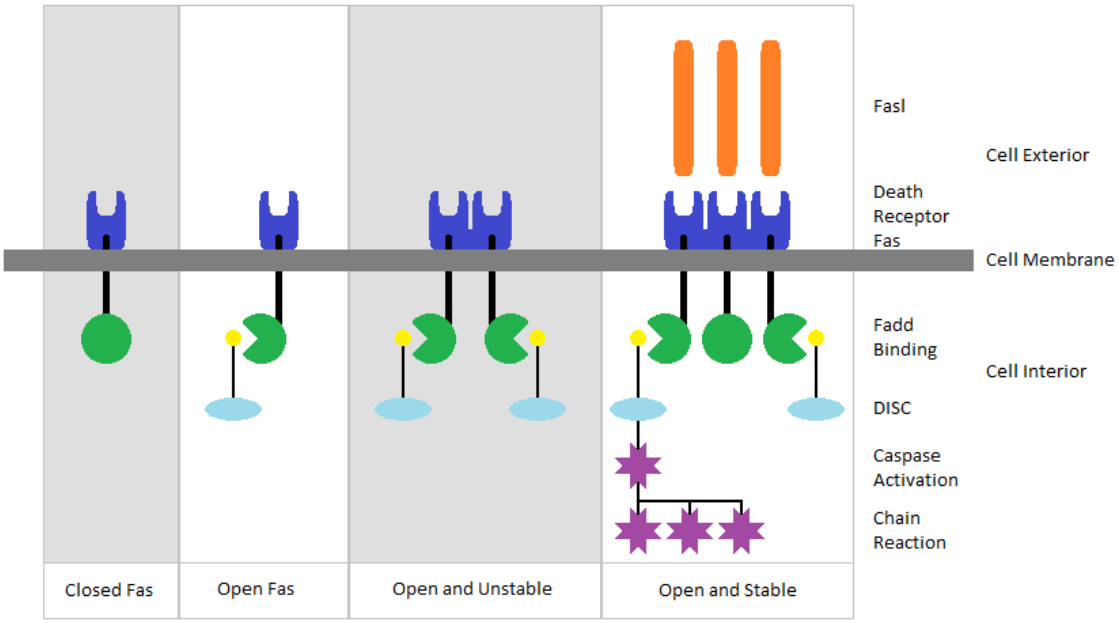

Figure 1: Extrinsic Pathway of Apoptosis

1.2 A review of mathematical models for clustering

The model by Lai and Jackson of death ligand-receptor dynamics assumes that FasL activates Fas by a direct link, then produces a DISC concentration that changes smoothly in relation to ligand input [17]. But the structural data by Scott and others[26] does not support the above assumption since Fas receptors were found in both closed and open forms. The open form allowed FADD binding and hence transduction of the apoptotic signal. Furthermore, open Fas receptors were observed to pair-stabilize through stem helix interactions. This allows a mechanism for bistability which resembles one observed in the Ising model[14]. In this model, once a certain threshold density of open Fas receptors is achieved, these open Fas receptors are able to sustain their conformations even after removal of the initial stimulus which promoted receptor opening. This produces hysteresis in the concentration of active, signaling receptors and therefore in apoptosis.

Our model assumes that FasL activates open and stable Fas receptors which drives the apoptotic signaling and the close Fas receptors is at equilibrium. The above model is represented by a scalar ordinary differential equation, which does produce the mechanism proposed by Ho and others[12]. Our assumption leads to these simplification of a system of equation use by Ho and other's model [12] to a scalar ordinary differential equation. The main idea is that FasL acts as a clustering platform for Fas, then induces contacts with other Fas through pairwise and higher-order interactions to form units capable of hysteresis. At low receptor concentrations, the model exhibits bistability provided that the number of receptors that each ligand can coordinate is at least three. Hence a theory for the trimeric character of FasL. Moreover, at high concentrations, irreversible bistability is achieved, implementing a permanent cell death decision. Therefore, the model supports a primary role for death receptors

in deciding cell fate. Additionally, our findings offer additional functional interpretations of ligand trimerism and receptor pre-association and localization within the unified context of bistability using bifurcational analysis.

1.3 Summary

Cancer may arise from disparity between the rates of cell growth and death in the body. The disparity can be triggered by mutations and hence disrupts apoptosis. We study the extrinsic pathway of apoptotic activation which is initiated upon detection of an external death signal, encoded by a death ligand, by its corresponding death receptor. Using the tools of mathematical analysis, we find that a model of death ligand-receptor interactions possesses the capacity for bistability. Therefore, the model supports threshold-like switching between life and death states and hence define a characteristic of an effective cell death mechanism. We thus describe the significant role of death receptors, the first component along the apoptotic pathway, in deciding cell fate. Furthermore, the model gives an explanation for a diverse biologically observed phenomena such as the trimeric character of the death ligand and the tendency for death receptors to occur together, in terms of bistability. The result quantifies the molecular basis of the apoptotic point-of-no-return.

Like in Ho's and others model[12], we assume the presence of both open and closed forms of Fas but only open and stable Fas receptors allows for FADD binding and promotion of apoptotic signaling. The closed form is the stable form and the open form is the unstable form of the Fas, see [25]. The Open Fas could pair up through stem helix interaction to self-stabilize.

Next, we describe Ho's and others model denoting each cluster by the tuple (L, X, Y, Z), L is FasL, and X, Y, and Z are three suggested forms of Fas: X

representing closed, Y representing receptors that are open and unstable, and Z representing receptors that are open and stable. Within each cluster, we define the reactions:

$$X \underset{k_c}{\overset{k_o}{\longleftrightarrow}} Y, \quad Z \xrightarrow{k_u} Y, \tag{1}$$

$$jY + (i-j)\,Z \xrightarrow{k_s^{(i)}} (j-k)\,Y + (i-j+k)\,Z, \quad \begin{cases} i = 2, \ldots, m, \\ j = 1, \ldots, i, \\ k = 1, \ldots, j, \end{cases} \tag{2}$$

$$L + jY + (i-j)\,Z \xrightarrow{k_l^{(i)}} L + (j-k)\,Y + (i-j+k)\,Z, \quad \begin{cases} i = 2, \ldots, n, \\ j = 1, \ldots, i, \\ k = 1, \ldots, j. \end{cases} \tag{3}$$

With the nondimensionalizations

$$\xi = \frac{x}{\rho}, \quad \eta = \frac{y}{\rho}, \quad \zeta = \frac{z}{\rho}, \quad \lambda = \frac{l}{\rho}, \quad \tau = k_c\, t, \tag{4}$$

following the convention that lowercase letters denote the concentrations of their uppercase counterparts, and where ρ is a characteristic concentration and t is time, and

$$\kappa_o = \frac{k_o}{k_c}, \quad \kappa_u = \frac{k_u}{k_c}, \quad \kappa_s^{(i)} = \frac{k_s^{(i)} s^{i-1}}{k_c}, \quad \kappa_l^{(i)} = \frac{k_l^{(i)} s^i}{k_c}. \tag{5}$$

Using Law of mass action, the following ordinary differential equations are obtained:

$$\begin{aligned}
\frac{d\xi}{d\tau} &= -\nu_o, \\
\frac{d\eta}{d\tau} &= \nu_o + \nu_u - \nu_s - \nu_l, \\
\frac{d\zeta}{d\tau} &= -\nu_u + \nu_s + \nu_l
\end{aligned} \tag{6}$$

where

$$\begin{aligned}
\nu_o &= \kappa_o \xi - \eta, \\
\nu_u &= \kappa_u \zeta, \\
\nu_s &= \sum_{i=2}^{m} \kappa_s^{(i)} \sum_{j=1}^{i} \eta^j \zeta^{i-j} \sum_{k=1}^{j} k, \\
\nu_l &= \lambda \sum_{i=2}^{n} \kappa_l^{(i)} \sum_{j=1}^{i} \eta^j \zeta^{i-j} \sum_{k=1}^{j} k.
\end{aligned} \tag{7}$$

For convenience, lets rename the nondimensional variables ξ, η, ζ, λ, and τ as x, y,z, l, and t respectively. For now, x, y, z, l, and t are considered nondimensionalized. It translates as follows:

$$\begin{aligned}
\frac{dx}{dt} &= -\nu_o, \\
\frac{dy}{dt} &= \nu_o + \nu_u - \nu_s - \nu_l, \\
\frac{dz}{dt} &= -\nu_u + \nu_s + \nu_l,
\end{aligned} \tag{8}$$

where

$$\begin{aligned}
\nu_o &= \kappa_o x - y, \\
\nu_u &= \kappa_u z, \\
\nu_s &= \sum_{i=2}^{m} \kappa_s^{(i)} \sum_{j=1}^{i} y^j z^{i-j} \sum_{k=1}^{j} k, \\
\nu_l &= l \sum_{i=2}^{n} \kappa_l^{(i)} \sum_{j=1}^{i} y^j z^{i-j} \sum_{k=1}^{j} k.
\end{aligned} \tag{9}$$

Using our hypothesis, which says close Fas is at the equilibrium. Then the first equation in Equation (8) reduces to an algebraic equation,

$$\kappa_o x - y = 0, \tag{10}$$

and using the assumption that $x + y + z = \sigma$. Ho and others model, Equation (8,9) reduces to our model which is a scalar ordinary differential equation

$$\frac{dz}{dt} = -\nu_u + \nu_s + \nu_l = P(z). \tag{11}$$

In chapter two, we talk about what the mathematical definition and mathematical preliminaries are about: linear and nonlinear equations, linearization, equilibrium points, bifurcation of equilibrium points, stability, invariant sets, hysteresis and Center Manifold Theorem. In chapter three, we analyze various cases of the model using stability analysis on the system. We show that the solutions are located in the positive cone and compute the number of possible positive solutions. In chapter four, we present the numerical simulations of the model. In chapter 5, we discuss our results and their conclusions.

CHAPTER 2

MATHEMATICAL PRELIMINARIES

In this chapter, we present definitions and mathematical preliminaries[23] that are relevant to chapter three.

The mathematical analysis of biological systems studies the stability of equilibria of the systems. In the apoptosis model(8,9) the stability conditions indicate the conditions where death and life states are feasible.

There are two methods of determining the stability of any system, Lyapunov stability analysis and linearization stability analysis. In this work, we use the linearization stability analysis in conjunction with phase plane analysis. To linearize is to approximate a function by a first-order Taylor series expansion about the equilibrium state. We linearize because we want the nonlinear system to behave more like a linear system, which makes it easier to determine stability in the neighborhood of the equilibrium point. We use the linearization method and deduce the stability of each equilibrium point.

The first thing to note is that system (8-9) has a well defined derivative. The vector field $\mathbf{f}$ of (8-9) is given by:

$$\frac{d\mathbf{x}}{dt} = \begin{bmatrix} \frac{dx}{dt} \\ \frac{dy}{dt} \\ \frac{dz}{dt} \end{bmatrix} = \begin{bmatrix} -\nu_o, \\ \nu_o + \nu_u - \nu_s - \nu_l, \\ -\nu_u + \nu_s + \nu_l \end{bmatrix} = \mathbf{f}(\mathbf{x}, \theta), \tag{12}$$

where $\theta = (\sigma, l)$ is the bifurcation parameter vector, and $\kappa_0, \kappa_s^i, \kappa_l^i$ are fixed. The

Jacobian matrix A of the vector field $\mathbf{f}$ is given by:

$$A = \frac{\partial \mathbf{f}}{\partial \mathbf{x}} = \begin{bmatrix} -\kappa_o & 1 & 0 \\ \kappa_0 & -1 - \nu_s^y - \nu_l^y & 1 - \nu_s^z - \nu_l^z \\ 0 & \nu_s^y + \nu_l^y & -1 + \nu_s^z + \nu_l^z \end{bmatrix},$$

where

$$\nu_l^y = \frac{\partial \nu_l}{\partial y}, \quad \nu_s^y = \frac{\partial \nu_s}{\partial y}, \quad \nu_l^z = \frac{\partial \nu_l}{\partial z}, \quad \nu_s^z = \frac{\partial \nu_s}{\partial z}.$$

The matrix elements of A are defined and continuous for all $\mathbf{x} \in \mathbb{R}^3$. Hence $\mathbf{f}$ is continuously differentiable, and the system of equations is well posed by Picards existence and uniqueness theorem, which at the minimum requires Lipschitz continuity. Next, we define an equilibrium point of equation system (8-9): the derivatives about the equilibrium point are given as

Definition 1 *If $f(\mathbf{x}_0, \theta)$=0 then $\mathbf{x}_0$ is an equilibrium point (also called a critical point or an equilibrium state solution) of the system equation (12).*

The equilibrium solutions of the system equation (12) are given by:

$$x_\star = \frac{\sigma - z_\star}{1 + \kappa_o}, \quad y_\star = \kappa_o x_\star,$$

where $\sigma = x + y + z$, and $z_\star$ is given by solving $\frac{dz}{dt} = 0$ with $(x, y) \mapsto (x_\star, y_\star)$, a polynomial, P in $z_\star$ of degree $\max\{m, n\}$.

To decide if each equilibrium point is stable or unstable, we first find the Jacobian of the matrix of the system (12). We linearize the nonlinear system (12) about the given equilibrium point, $\mathbf{x}_* = (x_*, y_*, z_*)$,

$$\frac{d\mathbf{x}}{dt} = A(\mathbf{x}_\star, \theta)(\mathbf{x} - \mathbf{x}_*). \tag{13}$$

Here A denotes the Jacobian of $\mathbf{f}$ and θ is a vector of parameters. Using the Jacobian enables us to linearize the non-linear systems around the equilibrium point.

If $\mathbf{x}_*$ is stable, the solution tends to move toward the equilibrium point, otherwise it is unstable. If the eigenvalues of the Jacobian are negatives, then it is stable. Otherwise, it is unstable.

The linearization of the vector field at an equilibrium point gives the following unique solution:

$$\mathbf{x}(t) = \exp(tA)\mathbf{x}(0)$$

Here $\exp(tA) = \sum_{n=0}^{\infty} \frac{t^n A^n}{n!}$. We say a non-zero vector $\mathbf{v}$ is an eigenvector of A with eigenvalue λ if $A\mathbf{v} = \lambda\mathbf{v}$. It is often the case that we can find a basis of eigenvectors $\mathbf{v}_1, ..., \mathbf{v}_n$ with eigenvalues $\lambda_1, ..., \lambda_n$. In this basis the matrix $exp(tA)$ becomes then a diagonal matrix with eigenvalues $e^{t\lambda_k}$ and we can read the behavior of the solutions of the linearized equation just by looking at the sign of the real parts of λ_k. Those with negative real parts, corresponding to special solutions with decay to zero with increasing time, are known as stable. Those with real parts equal to 0 correspond to constant or periodic solutions (depending on whether or not the imaginary part is zero or non-zero). Those with positive real parts, corresponding to solutions which diverge with increasing time, are known as unstable.

The eigenvalues of the jacobian from (12) are

$$0,\ \frac{A_1 - \sqrt{A_1^2 + 4A_2}}{2},\ \frac{A_1 + \sqrt{A_1^2 + 4A_2}}{2}$$

where

$$A_1 = -\kappa_o - 2 - a + b$$

$$A_2 = -a\kappa_o + \kappa_o b - 1 - b$$

and

$$a = \nu_s^y + \nu_l^y,\ b = \nu_s^z + \nu_l^z$$

In the next Chapter, we will show that the equilibrium solutions are in the positive cone if the polynomial P has a negative leading coefficient.

2.1 Invariant set

One of main goals of this work is to show the existence of an invariant set $\mathcal{C} \subset \mathbb{R}^3_+$. The existence assumes some additional conditions on the parameters.

Since the set $\mathcal{C}$ is a subset of the positive region of $\mathbb{R}^3$, we consider the flux of the system over the boundaries of the first octant in

$$\mathbb{R}^3, (ie.\{(i,j,k)|i,j,k \geq 0\}),$$

where the flux is given by the vector field $\mathbf{f}$ in (12). Introducing the hyperplanes $(x,y,0),(x,0,z),(0,y,z,)$ with outward directed unit normal vectors

$$\mathbf{n}_{z=0} = (0,0,-1), \;\; \mathbf{n}_{y=0} = (0,-1,0), \;\; \mathbf{n}_{x=0} = (-1,0,0),$$

respectively, one finds the outward flux over these surfaces is given by:

$$\begin{aligned}
\mathbf{f} \cdot \mathbf{n}_{x=0} &= -y, \\
\mathbf{f} \cdot \mathbf{n}_{y=0} &= -\kappa_o x - \kappa_u z, \\
\mathbf{f} \cdot \mathbf{n}_{z=0} &= -\nu_s - l \sum_{i=2}^{n} \kappa_l^{(i)} y^i \sum_{k=1}^{i} k.
\end{aligned}$$

The set $\mathcal{C}$ is clearly invariant with respect to the flow defined by the model if there is no outward flux. This imposes the conditions:

$$x \geq 0, \;\; y \geq 0, \;\; z \geq 0. \tag{14}$$

Note that the above condition gives us an unbounded region. We want conditions so that $\mathcal{C}$ is enclosed by a compact set. Since $x+y+z=\sigma$ for a solution $\mathbf{x}=(x,y,z)$ of Equation (8,9).

Therefore, the compact set $\{(x,y,z): x\geq 0, y\geq 0, z\geq 0, x+y+z=\sigma\}$ encloses the volume element $\mathcal{C}$. The unit normal vector to the surface $x+y+z=\sigma$ is given by

$$\mathbf{n}=(\frac{1}{\sqrt{3}},\frac{1}{\sqrt{3}},\frac{1}{\sqrt{3}}),$$

and the flux over these planes is given by:

$$\mathbf{f}\cdot\mathbf{n}=-\frac{\nu_o}{\sqrt{3}}+\frac{\nu_o+\nu_u-\nu_s-\nu_l}{\sqrt{3}}+\frac{-\nu_u+\nu_s+\nu_l}{\sqrt{3}}=0. \tag{15}$$

The results are summarized in the following theorem.

Theorem 2.1 *There exists an invariant set $\mathcal{C}$ with respect to the flow of system (12) given by*

$$\{(x,y,z): x\geq 0,\ y\geq 0,\ z\geq 0,\ x+y+z=\sigma\}.$$

2.2 Hysteresis

Hysteresis is a phenomenon that occurs in many processes [20]. We will show in the next chapter that the Equation (8,9) has an number of stable equilibrium points. The existence of multiple stable equilibria is closely related to hysteresis. This is a phenomenon that is often characterized by a looping behavior; however, the existence of a loop is not sufficient to identify hysteretic systems. We demonstrate that Equation (8,9) exhibits hysteresis. It is difficult to define hysteresis precisely but there is a common theme in defining hysteresis by identifying a looping behavior displayed

in the input-output map. There are many definitions of hysteresis available in the literature[20]. We consider hysteresis from a dynamical systems perspective.

Definition 2 *[20, Definition 3] A system exhibits hysteresis if it has*

(a) multiple stable equilibrium points and

(b) dynamics that are considerably faster than the time scale at which inputs are varied.

Condition (b) corresponds to the speed at which a controlled input is changed. In a lot of cases, hysteresis is present but is rate-dependent [20].

Definition 2 corresponds to the looping behavior which is often linked with hysteresis. Let us consider a system with two stable equilibria and suppose we start at the left equilibrium, see Figure 2a. If the input increases, the system will tend to stay in equilibrium, see Figure 2b, with only a small upward move along the hysteresis curve. When the input increases enough such that the equilibrium disappears, the system moves to the right equilibrium, see Figure 2c. This corresponds to moving along the steepest portion of the hysteresis loop. The system stays at the right equilibrium, see Figure 2d. If the input decreases enough so that the right equilibrium disappears, see Figure 2e, the system moves back to the left equilibrium, see Figures 2f and 2g. If the system moves to equilibrium faster than it changes in the input, the transition from one equilibrium to the other is nearly instantaneous and the system behavior can appear to be rate independent[20].

In our model for $m = 2, n = 2$, we show in Chapter 3 that Equation (12) has exactly one equilibrium, therefore the system for this case does not exhibit hysteresis by Definition 2.

The existence of a loop in the input-output map is not sufficient to define a system as hysteretic. In [20], they illustrate this by looking at a simple example of a damped second-order system

$$y''(t) + cy'(t) + ky(t) = u(t).$$

Differential Equation (16) satisfies Definition 2's requirement to exhibit hysteretic behavior.

Next, we investigate the following example

$$\frac{dx}{dt} = c + x - x^3 = f(x). \tag{16}$$

Lets find the equilibrium points by finding the roots of the equation $f(x) = c + x - x^3 = 0$. We can conclude that if the parameter c is positive or negative, there is exactly one root, $r(c)$. Now lets take the derivative when $c = 0$, which tells us that $f'(x) = -3x^2 + 1$ with respect to x at this root is negative, so this is a stable equilibrium point. Now lets take the derivative when $c < 0$ and $c > 0$. The derivative is negative with respect to x, so this is a stable equilibrium point. However, for the parameter $c \in (-2\sqrt{3}/3, 2\sqrt{3}/3)$ there are three equilibrium points. The middle point $c = 0$ is unstable, and the other two, $r(c)_- < r(c)_+$ are stable.

Let c have an initial value -100 at time 0. As c changes over time from -100 to 100, it follows one path, and as c changes over time from 100 to -100 it follows a different path.

2.3 Bifurcations of Equilibrium Points

Our system is dependent on a continuous parameter θ. Slight changes in θ result in slight changes to our system. When our system changes, the locations of equilibrium

points and their eigenvalues will also change. We will first illustrate this by tracking the movement of an equilibrium point x_θ by solving this equation, given by Definition 1:

$$f(x_\theta, \theta) = 0 \tag{17}$$

The implicit function theorem, see [11, 23] gives conditions for these solutions to exist for a small value of θ. We can differentiate the equation with respect to θ at $\theta = 0$ to obtain:

$$\partial_\theta F(x_0) + A\partial_\theta x = 0 \tag{18}$$

where the derivatives are evaluated at θ and the Jacobian matrix A is invertible. By the implicit function theorem the solution x_θ is unique for small θ. Now the condition that A is invertible can be stated as a condition that A not have zero as an eigenvalue, and so the only time that the number of equilibrium points can change is when the Jacobian matrix has 0 as an eigenvalue. The parameter values where the qualitative behavior of solutions changes are referred to as **critical thresholds**.

2.4 Center Manifold Theorem

Next, we discuss Center Manifold Theorem.

Theorem 2.2 *[23] Let* $\mathbf{f}$ *be a* C^r *vector field on* R^n *(i.e. it is continuous up to it's* r*th derivative) which vanishes at the origin (here the origin has been shifted to the equilibrium points). Suppose* $\mathbf{f}(0) = 0$ *and let* $A = D\mathbf{f}(0)$ *have* k *eigenvalues with a negative real part,* j *eigenvalues with a positive real part, and* $m = n-k-j$ *eigenvalues with a zero real part. Let the stable, center and unstable invariant subspaces be* E^s*,* E^c*, and* E^u *respectively. Then there exists* C^r *stable and unstable invariant manifolds*

W^s and W^u tangent to E^s and E^u at 0 and a $C^{(r-1)}$ center manifold W^c tangent to E^c at 0. The manifolds W^s, W^c, and W^u are invariant for the flow of $\mathbf{f}$.

Furthermore, the stable and unstable manifolds are unique but the center manifold need not be.

For an illustration of Center Manifold Theorem, we consider a simple non-linear system:

$$\dot{x}_1 = x_1^2, \tag{19}$$

$$\dot{x}_2 = -x_2, \tag{20}$$

$$\tag{21}$$

which we can rewrite as:

$$A = \begin{bmatrix} 0 & 0 \\ 0 & -1 \end{bmatrix},$$

Its eigenvalues are $\lambda = 0, \lambda = -1$ and corresponding eigenvectors $\begin{bmatrix} 1 \\ 0 \end{bmatrix}$ and $\begin{bmatrix} 0 \\ 1 \end{bmatrix}$; and

$$\mathbf{f}(x_1, x_2) = \begin{bmatrix} x_1^2 \\ -x_2 \end{bmatrix}.$$

Note that because $j = 0, k = 1, n = 2$, we determine that there are $m = n - k - j = 1$ eigenvalues with zero real part, and that there exists a center manifold $W^e(0)$ of class C^r tangent to the center subspace E.

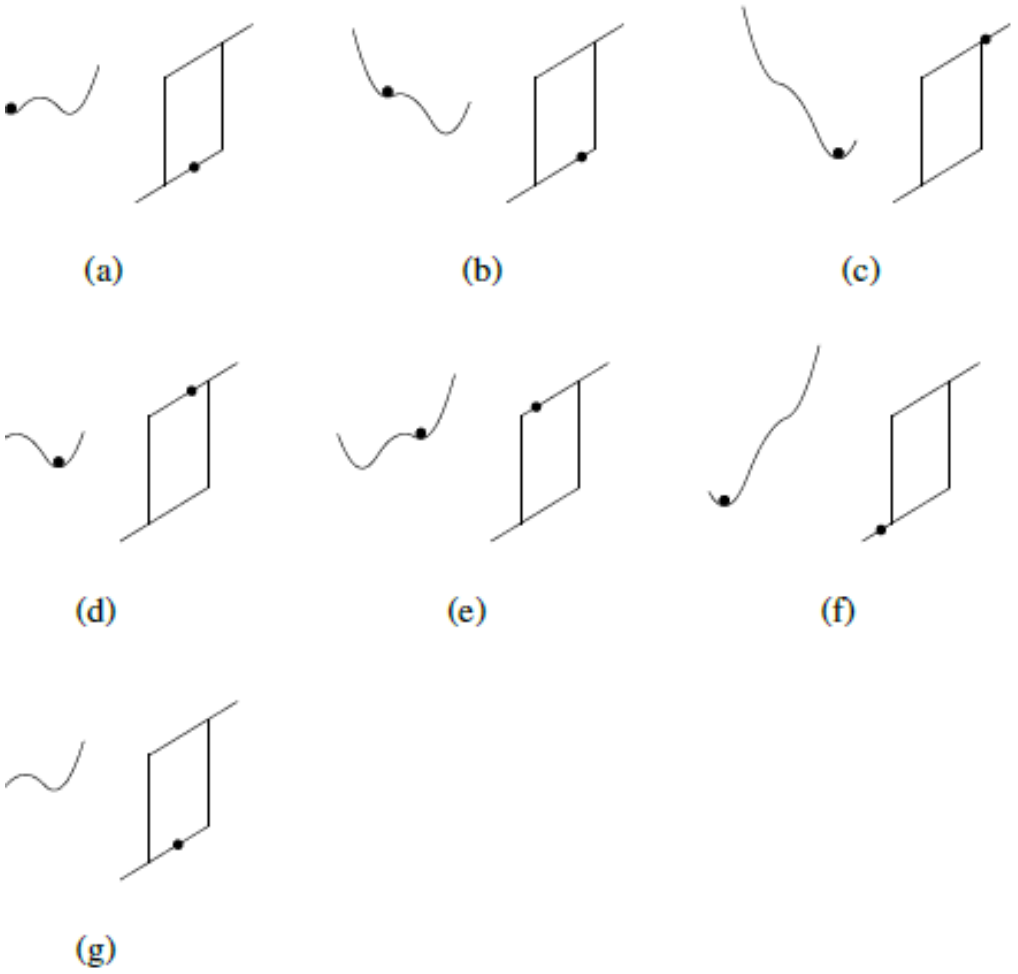

Figure 2: Dynamics of a system with two stable equilibria for a range of input values, and associated hysteresis loop.

CHAPTER 3

MATHEMATICAL MODEL

There are many mathematical models representing the interaction of Fas [26, 21]. As a reminder, our mathematical model is a simplification of Ho and other's model [12].

3.1 The Model

For convenience of the reader, we present again Equation (8-9) from Chapter 1. The main assumption in the model is that Fas exists in two forms: open and closed. In Ho's model [12], it was assumed that only open Fas allow for FADD binding and promote apoptotic signaling and this is supported by data. The closed form is the stable form and the open form is the unstable form of the Fas, see [25]. The open Fas could pair up through stem helix interaction to self-stabilize. We assume open stable Fas promote apoptotic signaling and close Fas is equilibrium state.

We label each cluster by the tuple (L, X, Y, Z), where L is FasL, and X, Y, and Z are three suggested forms of Fas: denoting closed receptors, open and unstable receptors, and open and stable receptors, respectively.

The parameters that m represents receptor density and n measures the coordination capacity of FasL. The concentration of molecules L, X, Y, Z are l, x, y, z respectively.

$$\begin{aligned} \frac{dx}{dt} &= -\nu_o, \\ \frac{dy}{dt} &= \nu_o + \nu_u - \nu_s - \nu_l, \\ \frac{dz}{dt} &= -\nu_u + \nu_s + \nu_l \end{aligned} \tag{22}$$

where

$$\begin{aligned}
\nu_o &= \kappa_o x - y, \\
\nu_u &= \kappa_u z, \\
\nu_s &= \sum_{i=2}^{m} \kappa_s^{(i)} \sum_{j=1}^{i} y^j z^{i-j} \sum_{k=1}^{j} k, \\
\nu_l &= l \sum_{i=2}^{n} \kappa_l^{(i)} \sum_{j=1}^{i} y^j z^{i-j} \sum_{k=1}^{j} k.
\end{aligned} \tag{23}$$

Since x, y, z are concentrations of molecules X, Y, Z, therefore, $x, y, z \geq 0$. Then the concentration values are in the non-negative octant which is known as the positive cone.

$$\mathbb{R}^3_+ \cup \{0,0,0\} = \{(x,y,z) | x \geq 0, y \geq 0, z \geq 0, \} \tag{24}$$

If we impose the assumption that Fas closed form is in equilibrium state equations (22,23) reduces to

$$\frac{dz}{dt} = -\nu_u + \nu_s + \nu_l = P(z), \tag{25}$$

where P is a polynomial in z.

Definition 3 *A surface set $S \subset R^3$ of $\frac{d\mathbf{x}}{dt} = \mathbf{f}(\mathbf{x}, \theta), \quad \mathbf{x}(t_0) = \mathbf{x}_0$ where $\mathbf{f}$ is continuously differentiable is called an invariant set of the system, if for all $\mathbf{x}_0 \in S$ and for all $t \geq 0, \mathbf{x}(t) \in S$.*

From Chapter 2, we know the positive cone is invariant under the system (22-23) and that there exists a compact invariant $\mathcal{C}$ set of the system in the positive cone. Hence $\mathbb{R}^+ \cup \{0\}$ is invariant under the Equation (25) and there is a compact invariant set of the Equation (25) in $\mathbb{R}^+ \cup \{0\}$.

Remark 1 *Note that the solution of the system (22-23) is non-negative and bounded in $\mathbb{R}^3$. Hence the solution of the scalar system is non negative and bounded in $\mathbb{R}$.*

3.2 Equilibria and Linear Analysis

In this section, we show the existence of equilibrium solutions in the positive cone of system (22-23), then this implies the existence of equilibrium solutions in $\mathbb{R}^+ \cup \{0\}$ of our scalar system (25).

Let $\mathbf{x}^* = (x^*, y^*, z^*)$ be an equilibrium of the system (22, 23). Then $\mathbf{x}^*$ is a solution the following algebraic system:

$$\begin{aligned} -\nu_o &= 0, \\ \nu_o + \nu_u - \nu_s - \nu_l &= 0, \\ -\nu_u + \nu_s + \nu_l &= 0. \end{aligned} \tag{26}$$

Note that

$$x^* + y^* + z^* = \sigma. \tag{27}$$

Hence

$$\begin{aligned} x^* &= \frac{y^*}{\kappa_o}, \\ y^* &= \frac{\kappa_o(\sigma - z^*)}{1 + \kappa_o}, \end{aligned} \tag{28}$$

and z^* is a root of the polynomial P, where

$$P(z) = -\kappa_u z + \sum_{i=2}^{m} \kappa_s^{(i)} \sum_{j=1}^{i} y^j z^{i-j} \sum_{k=1}^{j} k + l \sum_{i=2}^{n} \kappa_l^{(i)} \sum_{j=1}^{i} y^j z^{i-j} \sum_{k=1}^{j} k, \tag{29}$$

where

$$y = \frac{\kappa_o(\sigma - z)}{1 + \kappa_o}.$$

Note that the degree of the polynomial P is $\max\{m, n\}$ and

$$P(0) = \sum_{i=2}^{m} \kappa_s^{(i)} \sum_{j=1}^{i} \left(\frac{\kappa_o \sigma}{1 + \kappa_o}\right)^i \sum_{k=1}^{i} k + l \sum_{i=2}^{n} \kappa_l^{(i)} \sum_{j=1}^{i} \left(\frac{\kappa_o \sigma}{1 + \kappa_o}\right)^i \sum_{k=1}^{i} k > 0.$$

We need only to show that the polynomial P has at least one positive root with the help of Theorem 3.3 and Theorem 3.4.

Theorem 3.3 *[10] Let P be a polynomial of degree greater than 1 with the leading term negative and $P(0) > 0$, then the number of sign changes is odd.*

Proof: The proof follows from Descarte's rule .

Theorem 3.4 *Let P be a polynomial that satisfies Theorem 3.3, then the number of positive solutions is at least one and at most equal to the number of sign changes.*

Proof: The proof follows directly from Theorem 3.3.

The equilibrium solution of (22-23) is obtained by solving the follow algebraic system.

$$-\nu_o = 0, \tag{30}$$

$$-\nu_u + \nu_s + \nu_l = 0, \tag{31}$$

$$x + y + z = \sigma. \tag{32}$$

By Equation (30), we obtain

$$x = \frac{y}{\kappa_o}. \tag{33}$$

Then by using Equation (32), where σ is constant, we replace x with Equation (33) to obtain:

$$y = \frac{(\sigma - z)\kappa_o}{1 + \kappa_o}. \tag{34}$$

We obtain a polynomial in terms of z,

$$P(z) = -\kappa_u z + \sum_{i=2}^{m} \kappa_s^{(i)} \sum_{j=1}^{i} y^j z^{i-j} \sum_{k=1}^{j} k + l \sum_{i=2}^{n} \kappa_l^{(i)} \sum_{j=1}^{i} y^j z^{i-j} \sum_{k=1}^{j} k. \tag{35}$$

where y is as in Equation (34). Then the degree of the polynomial is $\max(n, m)$. We assume the leading coefficient of this polynomial is negative. Note that $P(0) > 0$

follows by the structure of the polynomial. Hence by Theorem 3.4, $P(z)$ has at least one positive solution and at most a number of positive solutions equal to number of sign changes.

We discuss in detail four different cases of our model, where (m,n) = (2,2), (3,2), (2,3), (3,3). We stop there because no new information will be obtained for cases where m or n are greater than three. Regardless, we discuss solutions of our model where (m,n) = (4,4) and (5,5) to create a stronger case for our hypothesis. This will be illustrated in Chapter 4. Let A_1 be the leading term and $P(0)$ is a constant term of the polynomial P. The parameters values are

$$k_0 = 0.002, k_u \ = 0.001, k_s^{(2)} = 0.1, k_l^{(2)} \ = 1, k_s^{(3)} = 0.5, k_l^{(3)} \ = 5$$

Model 1: $m = 2$ and $n = 2$

Given: $x + y + z = \sigma$, where σ is a constant and

$$x = \frac{y}{\kappa_o}.$$

we obtain

$$y = \frac{(\sigma - z)\kappa_o}{1 + \kappa_o}.$$

Then, we can write the polynomial P,

$$P(z) = -\kappa_u z + \sum_{i=2}^{m} \kappa_s^{(i)} \sum_{j=1}^{i} y^j z^{i-j} \sum_{k=1}^{j} k + l \sum_{i=2}^{n} \kappa_l^{(i)} \sum_{j=1}^{i} y^j z^{i-j} \sum_{k=1}^{j} k. \tag{36}$$

Using Maple, we find the leading coefficient A and the constant term C.

$$\begin{aligned} A_1 &= -\frac{(-2\kappa_o + 1)\kappa_o \kappa s^{(2)}}{(1 + \kappa_o)^2} - \frac{l(-2\kappa_o + 1)\kappa_o \kappa_l^{(2)}}{(1 + \kappa_o)^2}, \\ C = P(0) &= \frac{3\kappa_o^2 \sigma^2 \kappa_s^{(2)}}{(1 + \kappa_o)^2} + \frac{3\kappa_o^2 l \sigma^2 \kappa_l^{(2)}}{(1 + \kappa_o)^2}. \end{aligned} \tag{37}$$

Clearly, we see that $A < 0$ and that $C = P(0) > 0$. Therefore, using Theorem 3.4, the number of positive solutions of the polynomial $P(z) = Az^2 + Bz + C$ are as follows in the table below:

A	B	C	Number of Positive Solutions
-	+	+	1
-	-	+	1

Model 2: For $m = 3$ and $n = 2$ the polynomial P can be written as:

$$P(z) = -\kappa_u z + \sum_{i=2}^{m} \kappa_s^{(i)} \sum_{j=1}^{i} y^j z^{i-j} \sum_{k=1}^{j} k + l \sum_{i=2}^{n} \kappa_l^{(i)} \sum_{j=1}^{i} y^j z^{i-j} \sum_{k=1}^{j} k. \quad . \tag{38}$$

Using Maple, we find the leading coefficient A and the constant term D.

$$\begin{aligned} A &= -\frac{\kappa_s^{(3)}(4\kappa_o^2 - \kappa_o + 1)\kappa_o}{(1+\kappa_o)^3}, \\ D = P(0) &= \frac{3\sigma^2((l\kappa_l^{(2)} + 2\sigma\kappa_s^{(3)} + \kappa_s^{(2)})\kappa_o + l\kappa_l^{(2)} + \kappa_s^{(2)}\kappa_o^2)}{(1+\kappa_o)^3}. \end{aligned} \tag{39}$$

Again, we see that the leading coefficient $A < 0$ and the constant term $D = P(0) > 0$. Therefore, using Theorem 3.4, the number of positive solutions of the polynomial $P(z) = Az^3 + Bz^2 + Cz + D$ are as follows in the table below:

A	B	C	D	Number of Positive Solutions
-	+	+	+	1
-	+	-	+	3, 1
-	-	+	+	1
-	-	-	+	1

Model 3: For $m = 2$ and $n = 3$ the polynomial P can be written as follows:

$$P(z) = -\kappa_u z + \sum_{i=2}^{m} \kappa_s^{(i)} \sum_{j=1}^{i} y^j z^{i-j} \sum_{k=1}^{j} k + l \sum_{i=2}^{n} \kappa_l^{(i)} \sum_{j=1}^{i} y^j z^{i-j} \sum_{k=1}^{j} k. \tag{40}$$

Using Maple, we find the leading coefficient A and the constant term D.

$$\begin{aligned} A &= -\frac{l\kappa_o\kappa_l^{(3)}(4\kappa_o^2-\kappa_o+1)}{(1+\kappa_o)^3}, \\ D &= P(0) = \frac{3\kappa_o^2\sigma^2(2\kappa_o l\sigma\kappa_l^3+\kappa_o l\kappa_l^2+\kappa_o\kappa_s^2+l\kappa_l^2+\kappa_s^2)}{(1+\kappa_o)^3}. \end{aligned} \tag{41}$$

We see that the leading coefficient $A < 0$ and the constant term $D = P(0) > 0$. Therefore, using Theorem 3.4, the number of positive solutions of the polynomial $P(z) = Az^3 + Bz^2 + Cz + D$ are as follows in the table below:

A	B	C	D	Number of Positive Solutions
-	+	+	+	1
-	+	-	+	3, 1
-	-	+	+	1
-	-	-	+	1

Model 4: For $m = 3$ and $n = 3$ the polynomial P can be written as follows:

$$P(z) = -\kappa_u z + \sum_{i=2}^{m}\kappa_s^{(i)}\sum_{j=1}^{i}y^j z^{i-j}\sum_{k=1}^{j}k + l\sum_{i=2}^{n}\kappa_l^{(i)}\sum_{j=1}^{i}y^j z^{i-j}\sum_{k=1}^{j}k. \tag{42}$$

Using Maple, we find the leading coefficient A and the constant term D.

$$\begin{aligned} A &= -\frac{(4\kappa_o^2-\kappa_o+1)\kappa_o(l\kappa_l^{(3)}+\kappa_s^{(3)})}{(1+\kappa_o)^3}, \\ D &= \frac{6\kappa_o^2(((l\kappa_l^{(3)}+\kappa_s^{(3)})\sigma+\frac{l\kappa_l^{(2)}}{2}+\frac{\kappa_s^{(2)}}{2})\kappa_o+\frac{l\kappa_l^{(2)}}{2}+\frac{\kappa_s^{(2)}}{2})\sigma^2}{(1+\kappa_o)^3}. \end{aligned} \tag{43}$$

We see that the leading coefficient $A < 0$ and the constant term $D = P(0) > 0$. Therefore, using Theorem 3.4, the number of positive solutions of the polynomial $P(z) = Az^3 + Bz^2 + Cz + D$ are as follows in the table below:

A	B	C	D	Number of Positive Solutions
-	+	+	+	1
-	+	-	+	3, 1
-	-	+	+	1
-	-	-	+	1

Therefore, the table above shows that there exists at most three positive solutions and at least one positive solution.

Model 5: $m = 4$ and $n = 4$ the polynomial P can be written as follows:

$$P(z) = -\kappa_u z + \sum_{i=2}^{m} \kappa_s^{(i)} \sum_{j=1}^{i} y^j z^{i-j} \sum_{k=1}^{j} k + l \sum_{i=2}^{n} \kappa_l^{(i)} \sum_{j=1}^{i} y^j z^{i-j} \sum_{k=1}^{j} k. \tag{44}$$

Using Maple, we find the leading coefficient A and the constant term E.

$$A = \frac{(6\kappa_o^3 - 3\kappa_o^2 - 1)\kappa_o(l\kappa_l^{(4)} + \kappa_s^{(4)})}{(1+\kappa_o)^4},$$

$$E = P(0)\frac{1}{(1+\kappa_o)^4}(10(((l\kappa_l^{(4)} + \kappa_s^{(4)})\sigma^2 + (\frac{3l\kappa_l^{(3)}}{5} + \frac{3\kappa_s^{(3)}}{5})\sigma + \frac{3l\kappa_l^{(2)}}{10} + \frac{3\kappa_s^{(2)}}{10})\kappa_o^2$$
$$+((\frac{3l\kappa_l^{(3)}}{5} + \frac{3\kappa_s^{(3)}}{5})\sigma + \frac{3l\kappa_l^{(2)}}{5} + \frac{3\kappa_s^{(2)}}{5})\kappa_o + \frac{3l\kappa_l^{(2)}}{10} + \frac{3\kappa_s^{(2)}}{10})\sigma^2\kappa_o^2).$$

We see that the leading coefficient $A < 0$ and the constant term $E = P(0) > 0$. Therefore, using Theorem 3.4, the number of positive solutions of the polynomial $P(z) = Az^4 + Bz^3 + Cz^2 + Dz + E$ are as follows in the table below:

A	B	C	D	E	Number of Positive Solutions
-	+	+	+	+	1
-	+	+	-	+	3,1
-	+	-	+	+	3,1
-	+	-	-	+	3,1
-	-	+	+	+	1
-	-	+	-	+	3,1
-	-	-	+	+	1
-	-	-	-	+	1

Therefore, the table above shows that there exists at most three positive solutions and at least one positive solution.

Model 6:

$m = 5$ and $n = 5$ the polynomial P can be written as follows:

$$P(z) = -\kappa_u z + \sum_{i=2}^{m} \kappa_s^{(i)} \sum_{j=1}^{i} y^j z^{i-j} \sum_{k=1}^{j} k + l \sum_{i=2}^{n} \kappa_l^{(i)} \sum_{j=1}^{i} y^j z^{i-j} \sum_{k=1}^{j} k. \tag{45}$$

We see that the leading coefficient $A < 0$ and the constant term $F = P(0) > 0$. Therefore, using Theorem 3.4, the number of positive solutions of the polynomial $P(z) = Az^5 + Bz^4 + Cz^3 + Dz^2 + Ez + F$ are as follows in the table below:

A	B	C	D	E	F	Number of Positive Solutions
-	+	+	+	+	+	1
-	+	+	+	-	+	3,1
-	+	+	-	+	+	3,1
-	+	+	-	-	+	3,1
-	+	-	+	+	+	3,1
-	+	-	+	-	+	5,3,1
-	+	-	-	+	+	3,1
-	+	-	-	-	+	3,1
-	-	+	+	+	+	1
-	-	+	+	-	+	3,1
-	-	+	-	+	+	3,1
-	-	+	-	-	+	3,1
-	-	-	+	+	+	1
-	-	-	+	-	+	3,1
-	-	-	-	+	+	1
-	-	-	-	-	+	1

Therefore, the table above shows that there exists at most five positive solutions and at least one positive solution.

The Jacobian matrix of the system below:

$$\begin{aligned}
\frac{dx}{dt} &= -\kappa_o x + y, \\
\frac{dy}{dt} &= \kappa_o x - y + \kappa_u z - \sum_{i=2}^{m} \kappa_s^{(i)} \sum_{j=1}^{i} y^j z^{i-j} \sum_{k=1}^{j} k - l \sum_{i=2}^{n} \kappa_l^{(i)} \sum_{j=1}^{i} y^j z^{i-j} \sum_{k=1}^{j} k, \\
\frac{dz}{dt} &= -\kappa_u z + \sum_{i=2}^{m} \kappa_s^{(i)} \sum_{j=1}^{i} y^j z^{i-j} \sum_{k=1}^{j} k + l \sum_{i=2}^{n} \kappa_l^{(i)} \sum_{j=1}^{i} y^j z^{i-j} \sum_{k=1}^{j} k,
\end{aligned} \tag{46}$$

at the equilibrium point (x^*, y^*, z^*) is

$$J\mathbf{f}(x^*, y^*, z^*) = \begin{bmatrix} -\kappa_o & 1 & 0 \\ \kappa_o & -1 + a1 & \kappa_u + a3 \\ 0 & a2 & -\kappa_u + a4 \end{bmatrix}, \tag{47}$$

where

$$a1 = -\sum_{i=2}^{m} \kappa_s^{(i)} \sum_{j=1}^{i} (j) y_*^{j-1} z_*^{i-j} \sum_{k=1}^{j} k - l \sum_{i=2}^{n} \kappa_l^{(i)} \sum_{j=1}^{i} (j) y_*^{j-1} z_*^{i-j} \sum_{k=1}^{j} k,$$

$$a2 = \sum_{i=2}^{m} \kappa_s^{(i)} \sum_{j=1}^{i} (j) y_*^{j-1} z_*^{i-j} \sum_{k=1}^{j} k + l \sum_{i=2}^{n} \kappa_l^{(i)} \sum_{j=1}^{i} (j) y_*^{j-1} z_*^{i-j} \sum_{k=1}^{j} k,$$

$$a3 = -\sum_{i=2}^{m} \kappa_s^{(i)} \sum_{j=1}^{i} y_*^j (i-j) z_*^{(i-j)-1} \sum_{k=1}^{j} k - l \sum_{i=2}^{n} \kappa_l^{(i)} \sum_{j=1}^{i} y_*^j (i-j) z_*^{(i-j)-1} \sum_{k=1}^{j} k,$$

$$a4 = \sum_{i=2}^{m} \kappa_s^{(i)} \sum_{j=1}^{i} y_*^j (i-j) z_*^{(i-j)-1} \sum_{k=1}^{j} k + l \sum_{i=2}^{n} \kappa_l^{(i)} \sum_{j=1}^{i} y_*^j (i-j) z_*^{(i-j)-1} \sum_{k=1}^{j} k.$$

Note that $a2 = -a1$ and $a4 = -a3$.

The eigenvalues are found by solving Equation (48):

$$\begin{vmatrix} (-\kappa_o) - \lambda & 1 & 0 \\ \kappa_o & (-1 + a1) - \lambda & \kappa_u + a3 \\ 0 & -a1 & (-\kappa_u - a3) - \lambda \end{vmatrix} = 0. \tag{48}$$

Then Equation (48) becomes

$$(-\kappa_o - \lambda) \begin{vmatrix} (-1 + a1) - \lambda & \kappa_u + a3 \\ -a1 & (-\kappa_u - a3) - \lambda \end{vmatrix} - 1 \begin{vmatrix} \kappa_o & \kappa_u + a3 \\ 0 & (-\kappa_u - a3) - \lambda \end{vmatrix} = 0. \tag{49}$$

Hence,

$$(-\kappa_o - \lambda)[(-1 + a1 - \lambda)(-\kappa_u - a3 - \lambda) + a1(\kappa_u + a3)] - \kappa_o(-\kappa_u - a3 - \lambda) = 0. \quad (50)$$

We rewrite Equation (50) and get

$$-\lambda^3 + \lambda^2[-\kappa_o - 1 + a1 - \kappa_u - a3] + \lambda[a1\kappa_o - \kappa_u\kappa_o - a3\kappa_o - \kappa_u - a3] = 0. \quad (51)$$

Lets factor λ out of Equation (51) to obtain

$$-\lambda^2 + \lambda[-\kappa_o - 1 + a1 - \kappa_u - a3] + [a1\kappa_o - \kappa_u\kappa_o - a3\kappa_o - \kappa_u - a3] = 0. \quad (52)$$

Equation (52) is a quadratic equation

$$a\lambda^2 + b\lambda + c = 0, \quad (53)$$

where $a = -1$, $b = -\kappa_o - 1 + a1 - \kappa_u - a3$, and $c = a1\kappa_o - \kappa_u\kappa_o - a3\kappa_o - \kappa_u - a3$. Then the roots of this cubic polynomial are

$$\lambda = 0, \frac{b \pm \sqrt{b^2 - 4ac}}{2}. \quad (54)$$

Note that $a1 < 0$ and $a3 > 0$. Then $b < 0$ and $c < 0$. Since $ac > 0$, the discriminant $D = b^2 - 4ac$ is either smaller than b^2 or it is negative. If negative, solutions are complex with real part b, which is negative. Otherwise $\sqrt{|D|}$ must be still smaller $|b| = -b$, so that the two eigenvalues must still be negative. Either way, real parts of both non-zero eigenvalues must be negative. Thus the linearized system has one zero eigenvalue, and the other two eigenvalues have negative real parts.

The presence of a zero eigenvalue makes it impossible to apply linear stability analysis to the system. The nonlinear terms left out determine the stability. Hence

this requires the use of a nonlinear stability analysis theory such as the Lyapunov function. The characterization of equilibrium points will require using the Lyapunov function on the system. This is a challenging task in higher dimensions [23].

We know that linear stability analysis describes how a system behaves near an equilibrium point. But if we combine phase-plane analysis with linear stability analysis we can characterize the equilibrium points and hence the system dynamics. However, this approach is very difficult or impossible to implement in higher dimensions. Looking at the structure of our model, we see that it is equivalent to a one dimensional problem. Therefore, we study the equivalent one dimensional system

$$\frac{dz}{dt} = P(z) \tag{55}$$

where

$$P(z) = -\kappa_u z + \sum_{i=2}^{m} \kappa_s^{(i)} \sum_{j=1}^{i} y^j z^{i-j} \sum_{k=1}^{j} k + l \sum_{i=2}^{n} \kappa_l^{(i)} \sum_{j=1}^{i} y^j z^{i-j} \sum_{k=1}^{j} k,$$

and

$$y = \frac{(\sigma - z)\kappa_0}{1 + \kappa_0}.$$

We find the equilibrium points by solving $\frac{dz}{dt} = 0$ such that $P(z^*)$ is a polynomial in z^* of degree $\max\{m, n\}$. Note that the model is bistable only if $\max\{m, n\} \geq 3$, since two stable nodes must be separated by an unstable node as our model is effectively one-dimensional z.

We interpret z as a measure of the apoptotic activation of a cluster. We will illustrate this one dimensional problem in Chapter 4 using linear stability analysis and phase-plane analysis to characterize equilibrium states and hysteresis.

CHAPTER 4

NUMERICAL SIMULATION

For all the simulation in this Chapter, we use the following baseline parameter values

$$\sigma = 1, \kappa_o = 2 \times 10^{-3}, \kappa_u = 10^3$$

$$\kappa_s^(i) = (2i - 3) \times 10^{-1}, i = 2, 3, ...m$$

$$\kappa_s^(i) = (2i - 3) \times 10^{1}, i = 2, 3, ..., n.$$

and appropriate parameters $l \in [0, 0.5]$ and $\sigma \in [0.0, 4.0]$ to characterize the dynamics of the system producing apoptotic signaling. For $m = 2, n = 2$, the coefficients of the polynomial P are:

$$A = -0.0001984055840 - 0.001984055840(l),$$

$$B = -0.001 + 0.0001972103697(\sigma) + 0.001972103697(l)(\sigma),$$

$$C = P(0) = 1.195214362x10^{-6}(\sigma)^2 + 0.00001195214362(l)(\sigma).$$

From results in Chapter 2 and 3, we see that P has one positive root. Hence $z^* > 0$ has one equilibrium point, $Z^* > 0$ of the one dimensional ordinary differential equation system $\frac{dz}{dt} = P(z)$.

Next, we calculate equilibrium state activation curves for the Model for case $m = n = 2$. These curves exhibit monostability (see, Figures 3). This case does not capture the bistability mechanism and hysteresis since it has only one stable equilibrium. Figure 4 gives a more intuitive view of the dependence of the model's qualitative structure on l and σ.

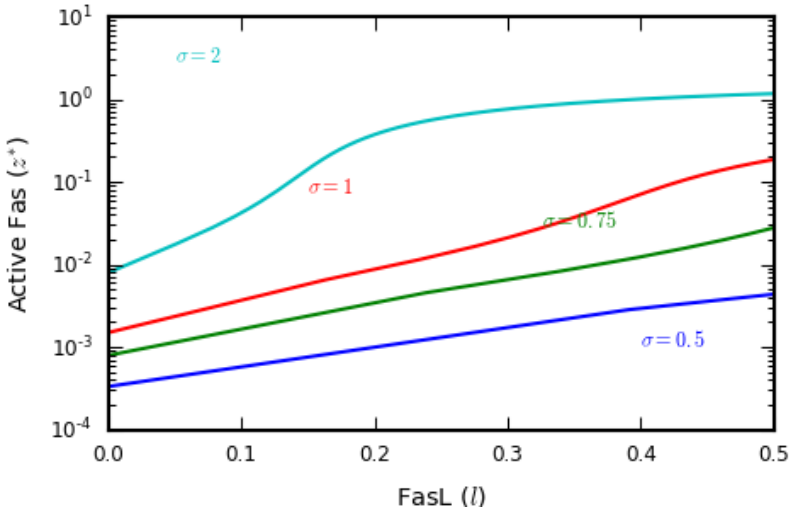

Figure 3: Equilibrium-state activation curves.

The equilibrium (steady)-state active Fas concentration z^* shows monostability as a function of the FasL concentration l. All parameters are set at baseline values.

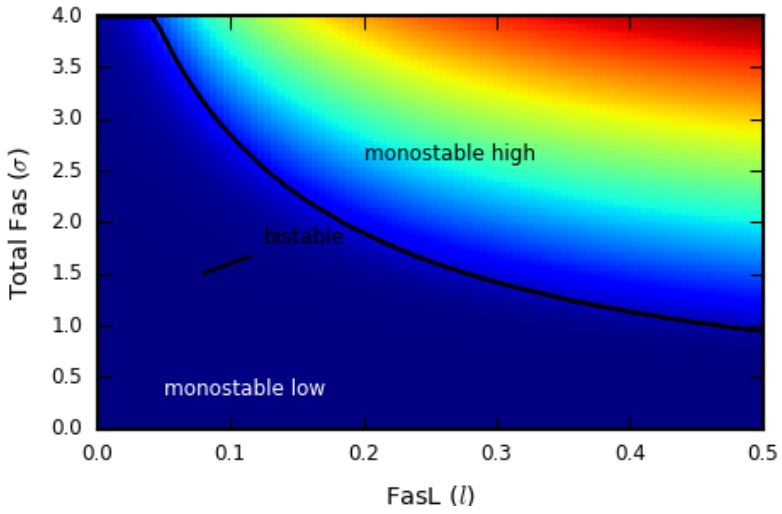

Figure 4: Equilibrium state diagram for the case $m = n = 2$.

In this simulation, we identify the regions of parameter space supporting monostability (colored) or bistability (gray) as a function of the FasL and total Fas concentrations l and σ, respectively. The monostable region is colored as a heat map corresponding to the equilibrium-state active Fas concentration z^*.

4.1 Classification Equilibrium-states

For cases of the model where $\max(m, n) \geq 3$, calculation of the equilibrium state activation curves shows that the model indeed exhibits bistability (see Figures 5-10) for suitable values of σ and l.

In all these cases, we confirm the bistability mechanism in extrinsic apoptosis. The associated hysteresis enables threshold switching between well separated low and high activation states. Biologically, this a programmed signal of life and death. These are integrated at the cell level to compute the overall apoptotic response.

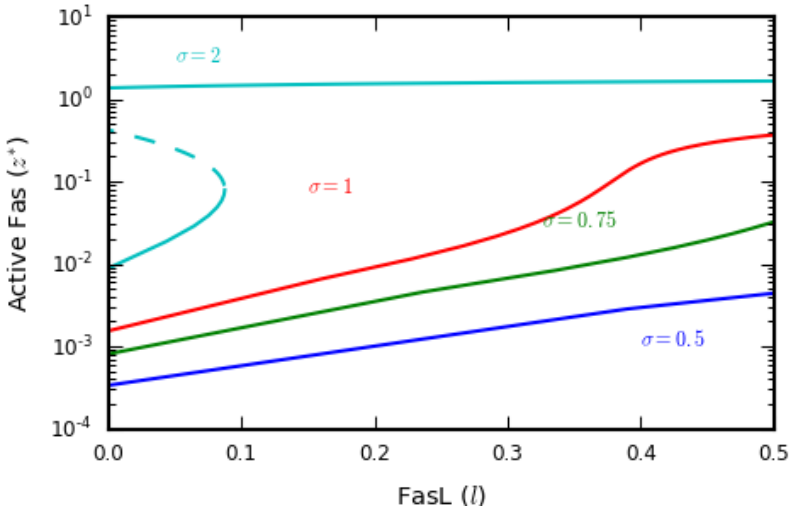

Figure 5: Equilibrium-state activation curves for the case $m = 3, m = 2$.

The equilibrium-state active Fas concentration z^* shows bistability and hysteresis as a function of the FasL concentration l (stable, solid lines; unstable, dashed lines). At low receptor concentrations σ, the bistability is reversible, but irreversibility emerges for σ sufficiently high, representing a committed cell death decision. All parameters are set at baseline values unless otherwise noted.

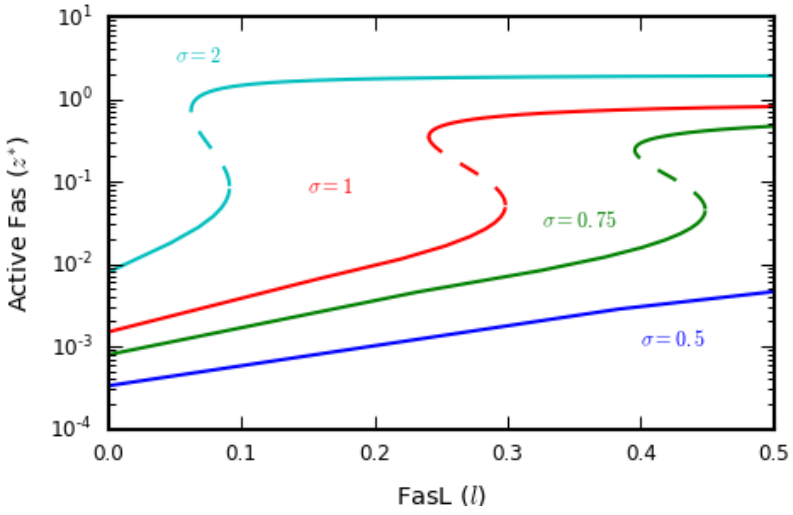

Figure 6: Equilibrium-state activation curves for the case $m = 2, m = 3$.

The equilibrium-state active Fas concentration z^* shows bistability and hysteresis as a function of the FasL concentration l (stable, solid lines; unstable, dashed lines). At low receptor concentrations σ, the bistability is reversible, but irreversibility emerges for σ sufficiently high, representing a committed cell death decision. All parameters ask set at baseline values unless otherwise noted.

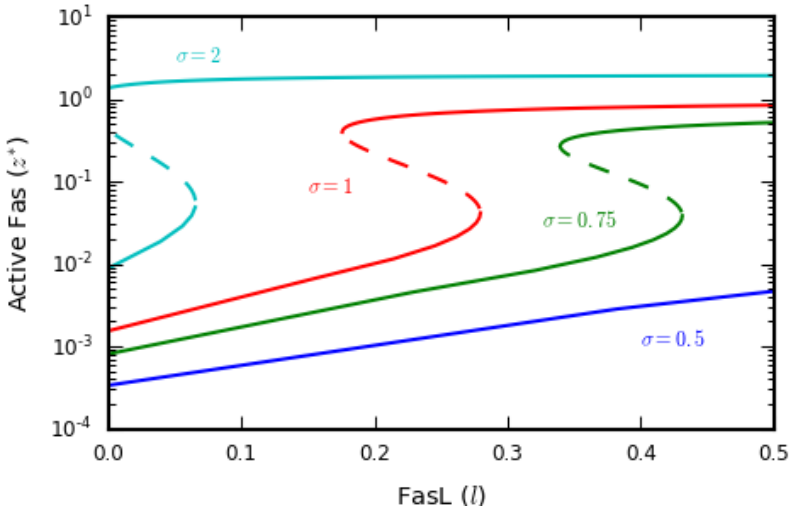

Figure 7: Equilibrium-state activation curves for the case $m = n = 3$.

The equilibrium-state active Fas concentration z^* shows bistability and hysteresis as a function of the FasL concentration l (stable, solid lines; unstable, dashed lines). At low receptor concentrations σ, the bistability is reversible, but irreversibility emerges for σ sufficiently high, representing a committed cell death decision. All parameters are set at baseline values unless otherwise noted.

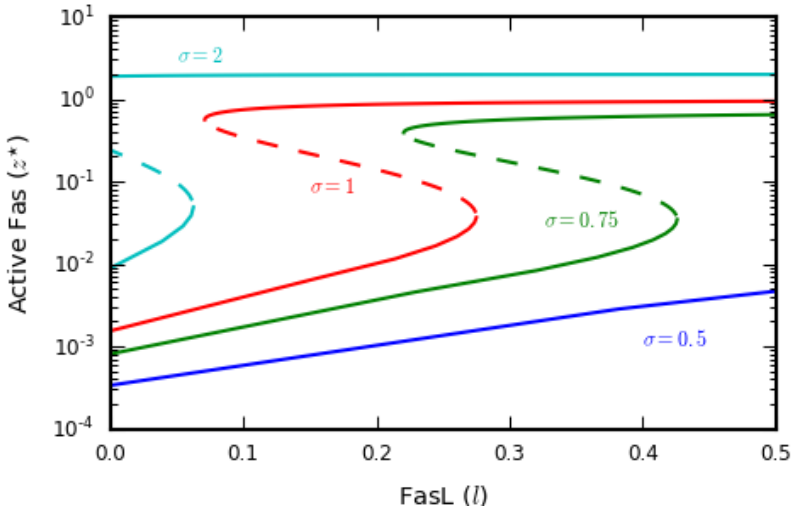

Figure 8: Equilibrium-state activation curves for the case $m = n = 4$.

The equilibrium-state active Fas concentration z^* shows bistability and hysteresis as a function of the FasL concentration l (stable, solid lines; unstable, dashed lines). At low receptor concentrations σ, the bistability is reversible, but irreversibility emerges for σ sufficiently high, representing a committed cell death decision. All parameters are set at baseline values unless otherwise noted.

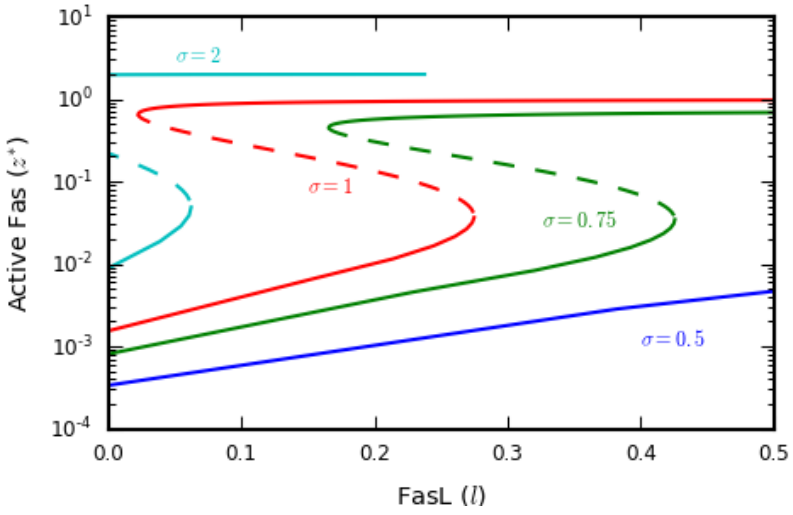

Figure 9: Equilibrium-state activation curves for the case $m = n = 5$.

The equilibrium-state active Fas concentration z^* shows bistability and hysteresis as a function of the FasL concentration l (stable, solid lines; unstable, dashed lines). At low receptor concentrations σ, the bistability is reversible, but irreversibility emerges for σ sufficiently high, representing a committed cell death decision. All parameters are set at baseline values unless otherwise noted.

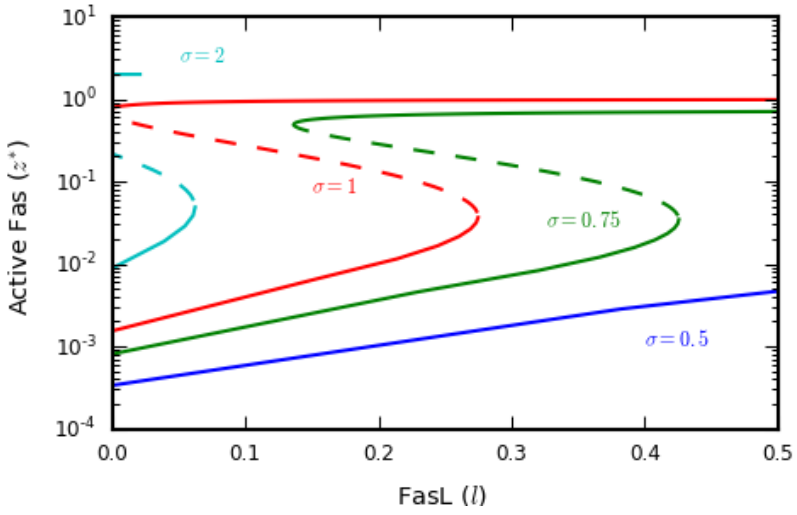

Figure 10: Equilibrium-state activation curves for the case $m = n = 6$.

The equilibrium-state active Fas concentration z^* shows bistability and hysteresis as a function of the FasL concentration l (stable, solid lines; unstable, dashed lines). At low receptor concentrations σ, the bistability is reversible, but irreversibility emerges for σ sufficiently high, representing a committed cell death decision. All parameters are set at baseline values unless otherwise noted.

Figures 11-16 give a more intuitive view of the dependence of the model's qualitative structure on l and σ.

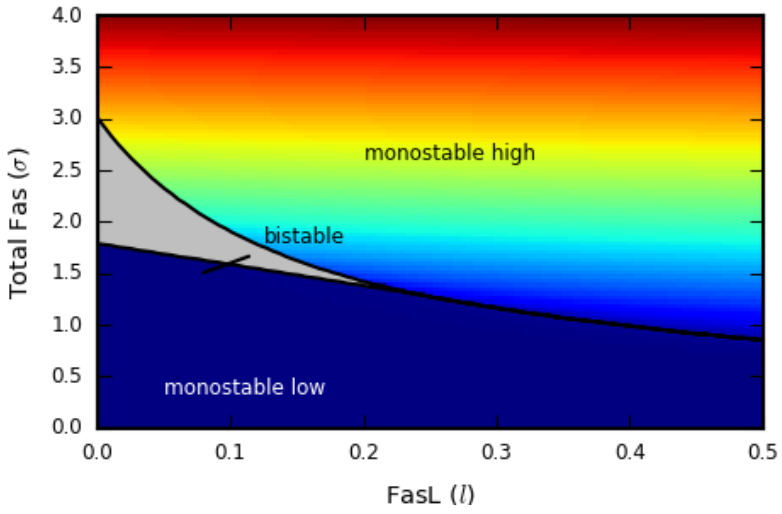

Figure 11: Equilibrium state diagram for the case $m = 3, n = 2$.

In this simulation, we identify the regions of parameter space supporting monostability (colored) or bistability (gray) as a function of the FasL and total Fas concentrations l and σ, respectively. The monostable region is colored as a heat map corresponding to the equilibrium-state active Fas concentration z^*.

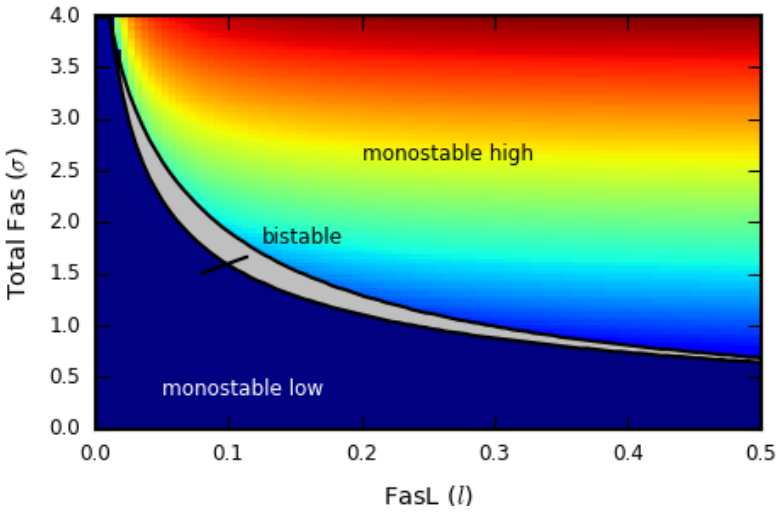

Figure 12: Equilibrium state diagram for the case $m = 2, n = 3$.

In this simulation, we identify the regions of parameter space supporting monostability (colored) or bistability (gray) as a function of the FasL and total Fas concentrations l and σ, respectively. The monostable region is colored as a heat map corresponding to the equilibrium-state active Fas concentration z^*.

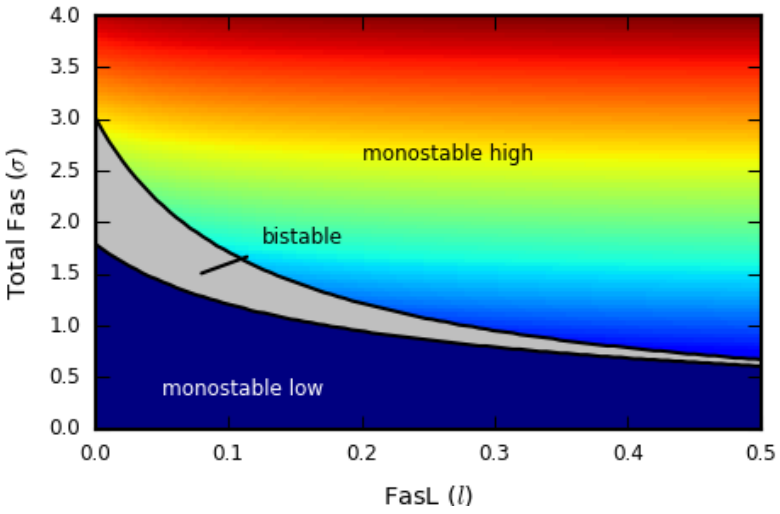

Figure 13: Equilibrium state diagram for the case $m = n = 3$.

In this simulation, we identify the regions of parameter space supporting monostability (colored) or bistability (gray) as a function of the FasL and total Fas concentrations l and σ, respectively. The monostable region is colored as a heat map corresponding to the equilibrium-state active Fas concentration z^*.

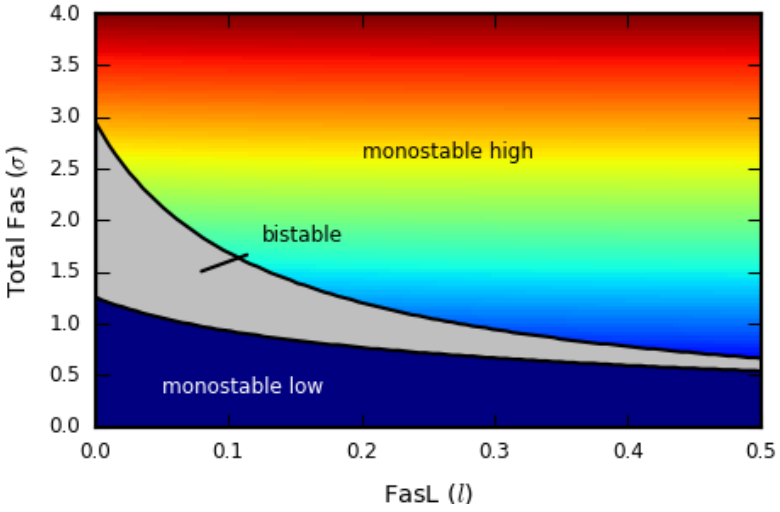

Figure 14: Equilibrium state diagram for the case $m = n = 4$.

In this simulation, we identify the regions of parameter space supporting monostability (colored) or bistability (gray) as a function of the FasL and total Fas concentrations l and σ, respectively. The monostable region is colored as a heat map corresponding to the equilibrium-state active Fas concentration z^*.

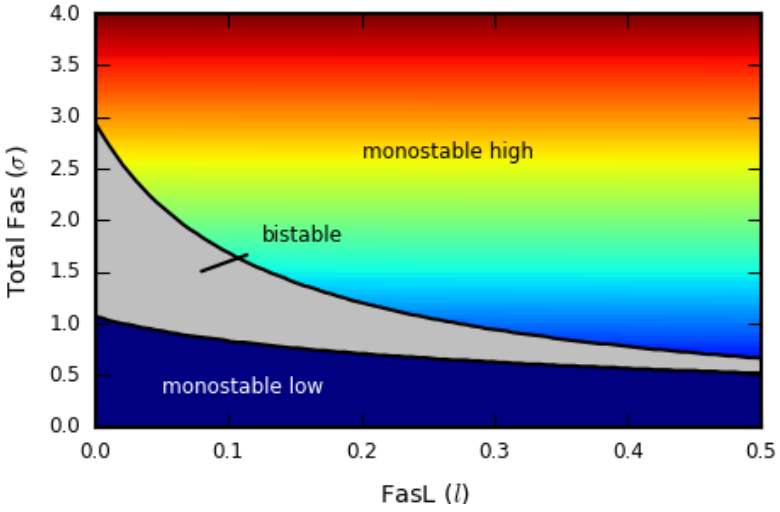

Figure 15: Equilibrium state diagram for the case $m = n = 5$.

In this simulation, we identify the regions of parameter space supporting monostability (colored) or bistability (gray) as a function of the FasL and total Fas concentrations l and σ, respectively. The monostable region is colored as a heat map corresponding to the equilibrium-state active Fas concentration z^*.

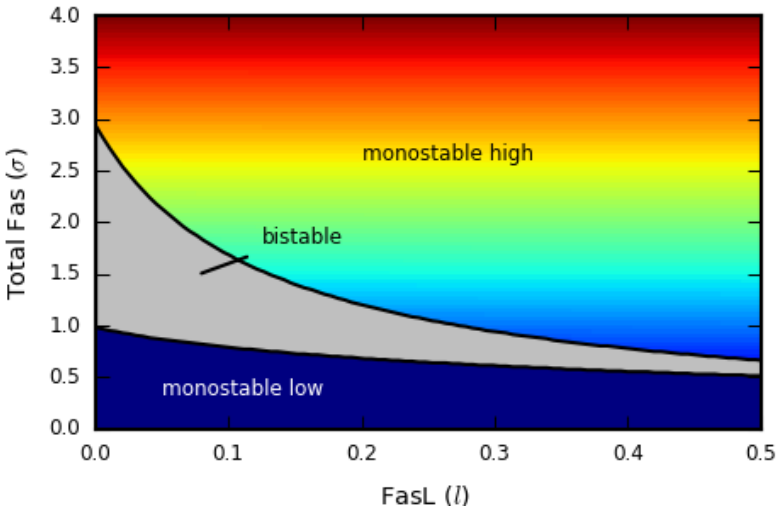

Figure 16: Equilibrium state diagram for the case $m = n = 6$.

In this simulation, we identify the regions of parameter space supporting monostability (colored) or bistability (gray) as a function of the FasL and total Fas concentrations l and σ, respectively. The monostable region is colored as a heat map corresponding to the equilibrium-state active Fas concentration z^*.

4.2 Hysteresis Curves

We now focus on the activation and deactivation thresholds l_+ and l_- respectively which define the bistable system. These are points at which the equilibrium state switches discontinuously from one branch to the other, and are given by values of l at which the hysteresis curve turns. These turns occur when $\frac{dl}{dz^*} = 0$ (see Figures 17-21).

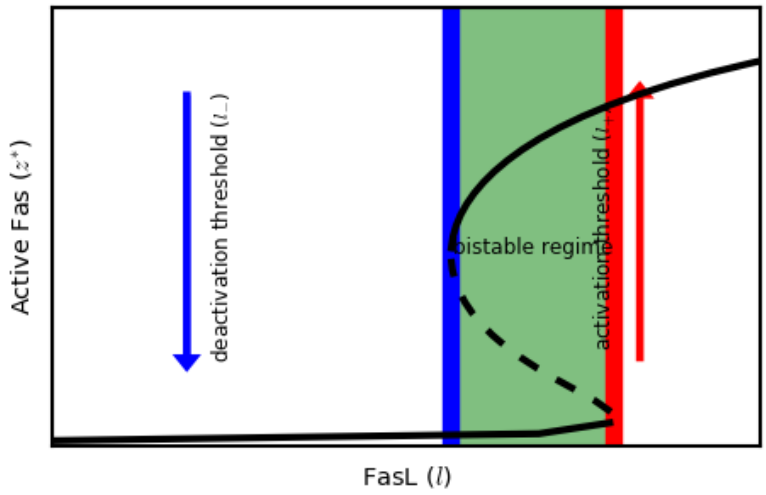

Figure 17: Bistability thresholds for the case $m = 2, n = 3$.

The activation (red) and deactivation (blue) thresholds $l_\pm$ characterizing the bistable regime (green) are defined as the concentrations l of FasL at which the equilibrium-state active Fas concentration z^* (black) switches discontinuously.

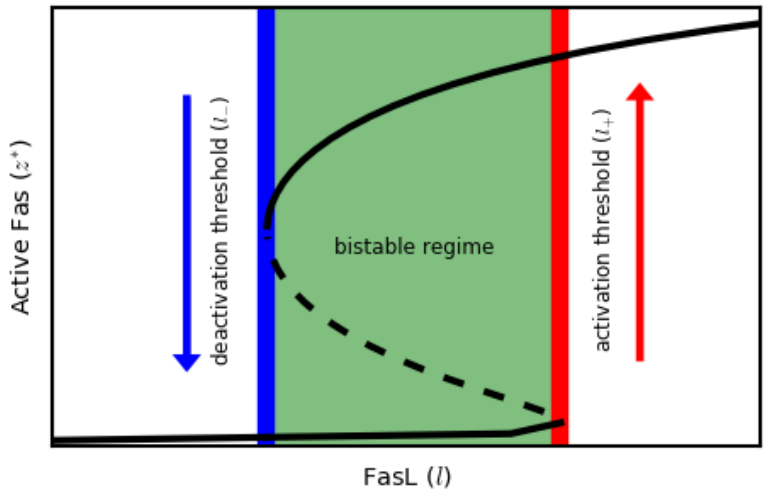

Figure 18: Bistability thresholds for the case $m = n = 3$.

The activation (red) and deactivation (blue) thresholds $l_\pm$ characterizing the bistable regime (green) are defined as the concentrations l of FasL at which the equilibrium-state active Fas concentration z^* (black) switches discontinuously.

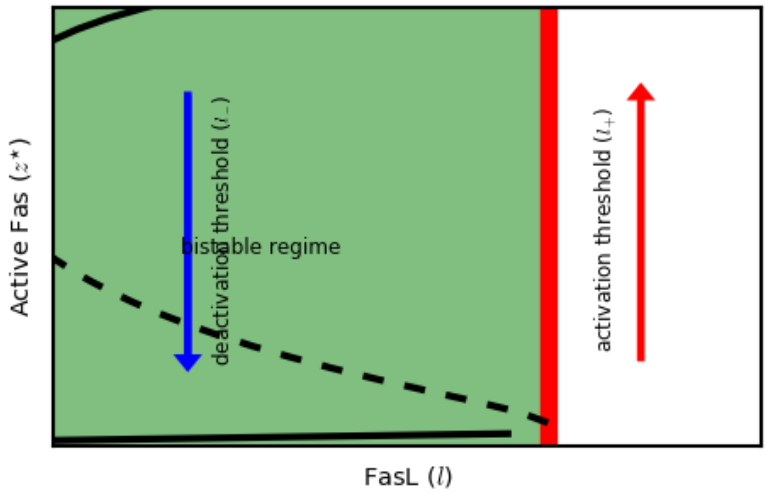

Figure 19: Bistability thresholds for the case $m = n = 4$.

The activation (red) and deactivation (blue) thresholds $l_\pm$ characterizing the bistable regime (green) are defined as the concentrations l of FasL at which the equilibrium-state active Fas concentration z^* (black) switches discontinuously.

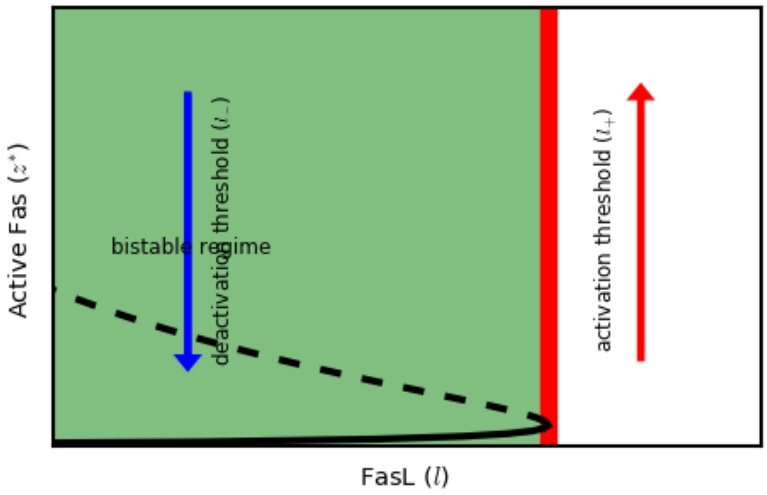

Figure 20: Bistability thresholds for the case $m = n = 5$.

The activation (red) and deactivation (blue) thresholds $l_\pm$ characterizing the bistable regime (green) are defined as the concentrations l of FasL at which the equilibrium-state active Fas concentration z^* (black) switches discontinuously.

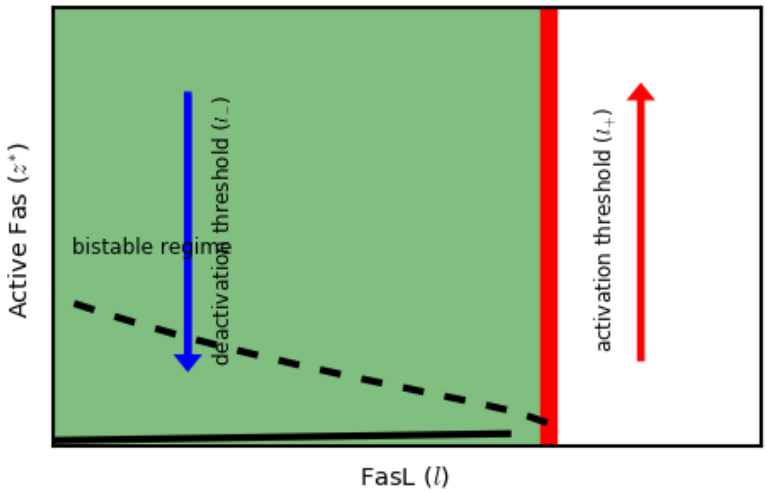

Figure 21: Bistability thresholds for the case $m = n = 6$.

The activation (red) and deactivation (blue) thresholds $l_\pm$ characterizing the bistable regime (green) are defined as the concentrations l of FasL at which the equilibrium-state active Fas concentration z^* (black) switches discontinuously.

We see that no new significant behaviors of the equilibrium-state activation curves are observed for either $m > 3$ or $n > 3$ (See Figures 5-10). Similarly, we can observe where equilibrium states are bistable (See Figures 4, 11-16). But when visualizing these systems by their thresholds, we do observe significant behaviors of bistability thresholds (See Figures 17-21).

CHAPTER 5

CONCLUSIONS AND DISCUSSIONS

We showed using the one dimensional equivalence of the model using linear stability analysis and phase-plane analysis of a nonlinear system of ordinary differential equations that receptor clustering does support bistability and hysteresis in apoptosis through a higher-order counterpart of biologically observed Fas pair-stabilization. The model also suggests that the signal processing activities are induced by receptor clustering. The results show that bistability plays a major functional role by enabling threshold switching between life and death states. Significantly, the analysis of the model indicates potential key roles for ligand trimerism and receptor pre-association. Thus, we can characterize insightful interpretations for these phenomena within the unified context of bistability. The model suggests an additional cell death decision, supplementing those that have been studied in the literature.

Critically, the proposed decision is implemented upstream at the very death receptors that initially detect the death signal encoded by FasL. This decision is therefore at the top in that it precedes all others in the system. Consequently, it operates independently of all intracellular components and so offers a general mechanism for bistability. Thus, receptor cluster-activation may explain how an effective apoptotic decision is implemented in such cells.

We believe that the model provides an interesting hypothesis for experimental biologists to test threshold of open Fas to induce apoptosis in a cell. The model does provide a real qualitative level. The significance of this work hence lies in its capacity to provide a hypothesis to test in future research. Also, looking at the Ho and other's model we see that the presence of the eigenvalues when we take Jacobian

of the system may be an artifact of having an incomplete model. We think that it is missing another hypothesis. We therefore readily invite experimentation which can support or add to our hypothesis.

WORKS CITED

[1] Albeck, John G, et al. "Modeling a Snap-Action, Variable-Delay Switch Controlling Extrinsic Cell Death." *PLoS Biology*, vol. 6, no. 12, 2 Dec. 2008.

[2] Albeck, John G., et al. "Quantitative Analysis of Pathways Controlling Extrinsic Apoptosis in Single Cells." *Molecular Cell*, vol. 30, no. 1, 11 Apr. 2008, pp. 11-25.

[3] Bagci, E.z., et al. "Bistability in Apoptosis: Roles of Bax, Bcl-2, and Mitochondrial Permeability Transition Pores." *Biophysical Journal*, vol. 90, no. 5, 1 Mar. 2006, pp. 1546-1559.

[4] Bentele, M., et al. "Mathematical Modeling Reveals Threshold Mechanism in CD95-Induced Apoptosis." *The Journal of Cell Biology*, vol. 166, no. 6, 13 Sept. 2004, pp. 839–851.

[5] Chauvet, Erica, et al. "A Lotka-Volterra Three-Species Food Chain." *Mathematics Magazine*, vol. 75, no. 4, Oct. 2002, p. 243.

[6] Cui, Jun, et al. "Two Independent Positive Feedbacks and Bistability in the Bcl-2 Apoptotic Switch." *PLoS ONE*, vol. 3, no. 1, 23 Jan. 2008.

[7] Eissing, Thomas, et al. "Bistability Analyses of a Caspase Activation Model for Receptor-Induced Apoptosis." *Journal of Biological Chemistry*, vol. 279, no. 35, 27 Aug. 2004, pp. 36892–36897.

[8] Fulda, S, and K-M Debatin. "Extrinsic versus Intrinsic Apoptosis Pathways in Anticancer Chemotherapy." *Oncogene*, vol. 25, no. 34, 7 Aug 2006, pp. 4798–4811.

[9] Fussenegger, Martin, et al. "A Mathematical Model of Caspase Function in Apoptosis." *Nature Biotechnology*, vol. 18, no. 7, 18 July 2000, pp. 768–774.

[10] Grabinar, David J. "Descartes' Rule of Signs: Another Construction". *The American Mathematical Monthly*, vol. 106, no. 9, Nov. 1999, pp. 854–856.

[11] Hale, Jack K., and Kocak Huseyin. *Dynamics and Bifurcations*. Springer, 1991.

[12] Ho, Kenneth L., and Heather A. Harrington. "Bistability in Apoptosis by Receptor Clustering." *PLoS Computational Biology*, vol. 6, no. 10, 14 Oct. 2010.

[13] Hua, F., et al. "Effects of Bcl-2 Levels on Fas Signaling-Induced Caspase-3 Activation: Molecular Genetic Tests of Computational Model Predictions." *The Journal of Immunology*, vol. 175, no. 2, 15 July 2005, pp. 985-995.

[14] Ising E. "Beitrag zur theorie des ferromagnetismus." *Z Phys*, vol. 31, Feb. 1925, pp. 253–258.

[15] Kerr, J F R, et al. "Apoptosis: A Basic Biological Phenomenon with Wide-ranging Implications in Tissue Kinetics." *British Journal of Cancer*, vol. 26, no. 4, Aug. 1972, pp. 239-257.

[16] Kitano, Hiroaki. "Biological Robustness." *Nature Reviews Genetics*, vol. 5, no. 11, 1 Nov. 2004, pp. 826–837.

[17] Lai R, Jackson TL. "A Mathematical Model of Receptor-Mediated Apoptosis: Dying to Know Why FasL is a Trimer." *Math Biosci Eng*, vol. 1, Sept. 2004, pp. 325–328.

[18] Legewie, Stefan, et al. "Mathematical Modeling Identifies Inhibitors of Apoptosis (IAPs) as Mediators of Positive Feedback and Bistability." *PLoS Computational Biology*, vol. 2, no. 9, 15 Sept. 2006.

[19] Meier, Pascal, et al. "Apoptosis in Development." *Nature*, vol. 407, no. 6805, 12 Oct. 2000, pp. 796-801.

[20] K. Morris. "What is hysteresis?" *Applied Mechanics Reviews*, vol. 64, no. 5, Sept 2011.

[21] Muppidi JR, Siegel RM. "Ligand-independent redistribution of Fas (CD95) into lipid rafts mediates clonotypic T cell death." *Nat Immunol*, vol. 5, no. 2, Feb. 2004, pp.182–189.

[22] Okazaki, Noriaki, et al. "Simple Computational Models of Type I/Type II Cells in Fas Signaling-Induced Apoptosis." *Journal of Theoretical Biology*, vol. 250, no. 4, 21 Feb. 2008, pp. 621-633.

[23] Perko, L. *Differential Equations and Dynamical Systems*. Springer-Verlag New York, 2012.

[24] Raff, Martin. "Cell Suicide for Beginners." *Nature*, vol. 396, no. 6707, 12 Nov. 1998, pp. 119–122.

[25] Salvesen, Guy S., and Stefan J. Riedl. "Structure of the Fas/FADD Complex: A Conditional Death Domain Complex Mediating Signaling by Receptor Clustering." *Cell Cycle*, vol. 8, no. 17, 1 Sept. 2009, pp. 2723–2727.

[26] Scott FL, Stec B, Pop C, Dobaczewska MK, Lee JJ, et al. "The Fas-FADD death domain complex structure unravels signalling by receptor clustering". *Nature* vol. 457, no. 7232, 19 Feb. 2009, pp. 1019–1022.

[27] Smoller, Joel. *Shock Waves and Reaction-Diffusion Equations*. Springer-Verlag New York Inc., 2012.

[28] Taylor, Rebecca C., et al. "Apoptosis: Controlled Demolition at the Cellular Level." *Nature Reviews Molecular Cell Biology*, vol. 9, no. 3, 9 Mar. 2008, pp. 231–241.

[29] Thompson, C. "Apoptosis in the Pathogenesis and Treatment of Disease." *Science*, vol. 267, no. 5203, 10 Mar. 1995, pp. 1456–1462.

[30] Zill, Dennis G. *A First Course in Differential Equations*. Brooks/Cole, 2001.